
3 INSTRUMENTATION

3.1 Introduction

This chapter details the apparatus and instrument configurations employed for each experimental study conducted as part of this thesis. The aim is to describe the experiments and justify why the different systems were employed. The chapter itself can be considered in two halves. The first half detailing the provision of consumables, how they were generated and managed, key apparatus and the separate sample introduction methods employed. While the second half specifically details the experiments undertaken (centred on the case studies first described in Section 1.1.2), along with blank and stability studies as appropriate.

3.1.1 Overview of experiments

Two experiments are described in this chapter. Table 3.1 introduces each one with a brief overview of the objectives and key apparatus used.

Table 3.1 List of experiments

Experiment	Objective	Key apparatus	Section
1: Parameter study	Investigate effect of varying pressure, humidity and magnitude of flow upon the detection of dimethylmethylphosphonate by an Owlstone Lonestar unit	<ul style="list-style-type: none"> • Permeation source • Owlstone Lonestar 	3.5
2: Detecting ethyl acetate in wine	Investigate ability to detect ethyl acetate within wine	<ul style="list-style-type: none"> • Gas chromatography • Owlstone FSIMS unit 	3.6

3.2 Consumables and gauges

Both of the experiments listed within Table 3.1 required gas supplies and subsequent management of pressures, hydrocarbon and humidity content. This section describes the origin of these gas supplies and the flow paths employed to ensure they were suitable for the investigations.

Additionally, variation in the pressure of a carrier flow necessitated manual pressure and flow gauges. Descriptions of these units and the ranges that they were operated are also included.

3.2.1 Gas supply - air

Air is a common carrier gas for FAIMS studies since the presence of both molecular nitrogen and oxygen allows the formation of positive and negative reactant ions (Section 2.2). In both of the experiments within Table 3.1 air was required at one or more points. Within the laboratory the air was fed through to the apparatus via a compressed air supply (Jun Air Compressor 25MD3) and Zero Air Generator (Texol ZA40). This produced 40 l/min of air at a gauge pressure of 4.14 bar (~ 400 kPa) and humidity of 10 ppm (monitored

constantly via a Cermet 2 Hygrometer). The capability of the Zero Air Generator was the removal of hydrocarbons to a 0.1 ppm methane level at 40 l/min.

3.2.2 Gas supply - nitrogen

Grade 5 nitrogen (99.999%, BOC) was used as the mobile phase within the gas chromatograph (GC) deployed in Experiment 2 (Table 3.1). Through the Golay equation [1] the diffusion and mass transfer through a GC column can be used to calculate the range of flow rates which permit maximum efficiency. This flow rate range is dependent upon the carrier gas used and of the three commonly employed (hydrogen, helium and nitrogen) nitrogen has the smallest flow rate range. However, nitrogen was selected for Experiment 2 because the flow from the column was to be later mixed with a carrier gas of air for a FAIMS unit. The potential loss of maximum resolution within the GC separation was deemed preferable to introducing an additional chemical compound that was not already present within the ionisation region of the FAIMS unit.

3.2.3 Pressure regulation

Pressures of laboratory gas supplies were regulated to the various experiments that were conducted concurrently within the laboratory. Additional pressure regulation was then implemented prior to each individual experiment. The locations of pressure management within individual experiments are included within Sections 3.5 - 3.6. The pressure regulator employed was the SMC Precision Regulator (IR1000-FO1B) which has a pressure range up to 0.2 MPa in 0.01 MPa gauge increments.

3.2.4 Flow controllers and meters

Within Experiments 1 and 2 (Table 3.1) flow controllers were used in-line and constantly while flow meters were used prior to data acquisition in order to confirm the flow to a unit. The flow controllers used were either the FJC-625-040F flow meter for air (Fisher Scientific) or P16S4-TH0 flow meter (Aalborg). They were capable of controlling flows between $0.3 - 3 \pm 0.1$ l/min and $0 - 10 \pm 0.25$ l/min respectively. The flow meters used were either the GFM mass flow meter (Aalborg) or Flowmeter 6000 (Restek). They were capable of measuring flows of $0 - 5$ l/min $\pm 1.5\%$ and $0 - 500$ ml/min $\pm 2.5\%$ respectively.

In addition, mass flow controllers (MFCs), made in-house at Owlstone, were commonly utilised to control flows into an experimental set-up. Central to the design is an Aalborg mass flow controller. The MFC is to a large extent an Owlstone vapour generator (Section 3.4.1) without the permeation oven or temperature control.

3.2.5 Management of humidity and volatiles

Since the response from a FAIMS device is dependent upon the compounds which enter the unit (Sections 1.5 and 2.2) it is important that unwanted volatile compounds and humidity are removed from the carrier flow. This was accomplished for both experiments through the use of activated charcoal scrubbers which housed Descotec AirPel (10p2z25) and 13X molecular sieves (Sigma Aldrich) which would trap volatiles and humidity respectively.

An independent humidity sensor (Michell Instruments) was occasionally employed to discover the humidity of individual experimental flows; measurement range -100 to 20°C dew point.

3.2.6 Flow path

Linking the separate units was principally achieved by polytetrafluoroethylene (PTFE) tubing of 1/8" outer diameter. PTFE is chemically inert and its flexibility was extremely practical (some experiments had to be relocated between testing).

Particular parts of the flow path were, however, deemed unsuitable for PTFE; these were typically where analyte introduction took place, heated parts of the flow path and prior to a FAIMS unit. In these cases stainless steel was used. Within the experimental set-ups, detailed later, heated unions are highlighted and the flow path in these regions was stainless steel.

3.3 Key apparatus

Within Table 3.1 a column of key apparatus was included. The units central to the investigations are presented in turn below, while further details of the sample introduction methods are provided in Section 3.4.

3.3.1 Lonestar unit

The Owlstone Lonestar (LNS, Figure 3.1) was developed as a flexible stand alone FAIMS unit for investigations into a wide range of applications [2, 3]. Table 3.2 provides some of the general properties of the Owlstone Lonestar unit. The carrier gas can be extracted from ambient air and following passage through a scrubber is passed through to the FAIMS sensor. A separate inlet draws a reduced sample volume which is added to the main flow path prior to the ionisation region of the FAIMS sensor, presented later in Figure 3.2. If a

gas supply for the carrier flow is available the Lonestar unit utilises common Swagelok fittings so that a more characterised carrier gas can also be used in the laboratory.

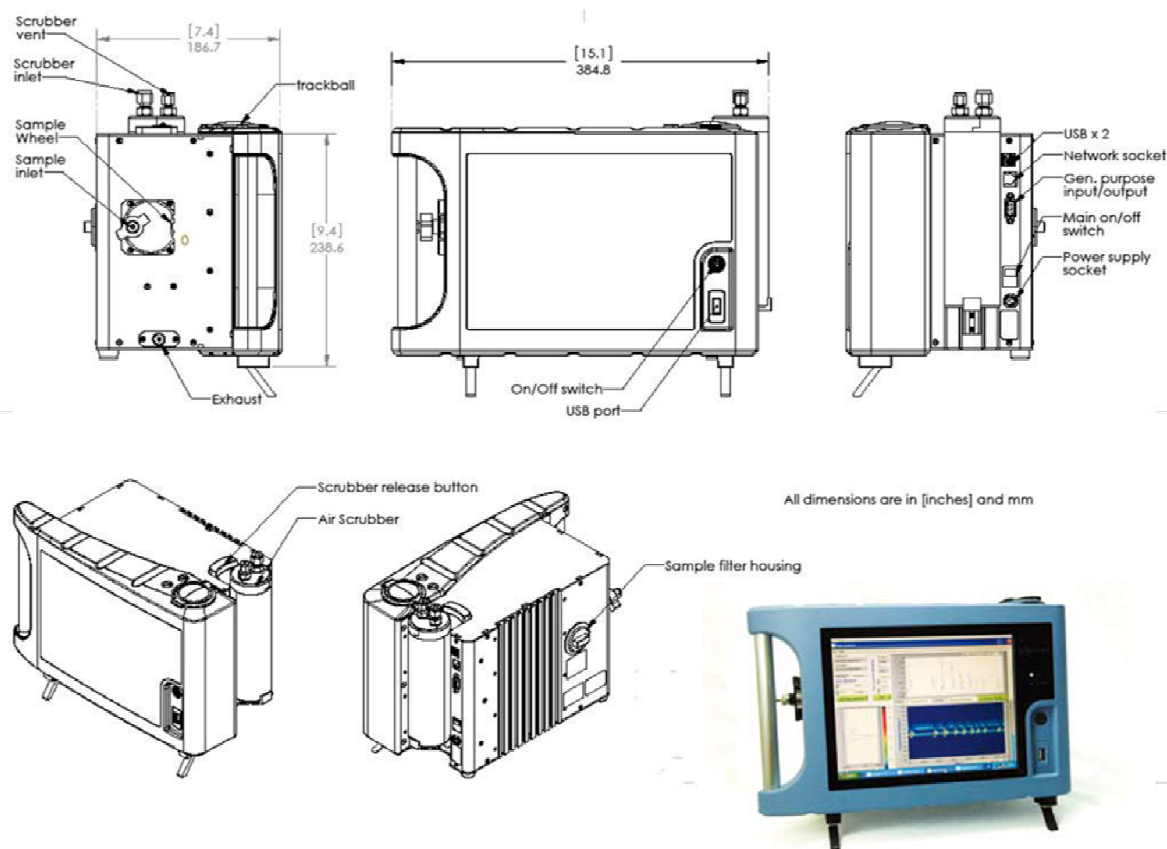


Figure 3.1 Owlstone Lonestar unit (LNS).

The unit houses an integrated computer, which enables the Labview software to be run without an additional laptop or external PC. Apart from data acquisition the onboard software was not utilised within this thesis and the data were exported to bespoke programs (Matlab) detailed within Chapters 4 - 6. Control of the unit can be performed exclusively via an integrated roller ball but USB ports allow for a mouse and keyboard to be used as well. A Faraday cup is used to detect the ions that pass through the drift region of the FAIMS sensor.

Table 3.2 Technical specifications of Owlstone Lonestar (as taken from Owlstone Ltd data sheet [2])

Characteristic	Property
Technology	Field asymmetric ion mobility spectrometry (FAIMS)
Detection mode	Positive and negative ions
Sample input	Ambient, headspace, process line
Inlet / outlet	1/8 inch Swagelok compression fittings
Analyte range	Industrial gases, VOCs, warfare simulants
Dynamic range	User adjustable inlet dilution for ppb -% concentrations
Instrument air	Integrated and easy-to-replace scrubber and desiccant connection to air line for long life, fixed point operation
Max heater temperature	70°C (343 K)
Humidity range	0% - 95%
Instrument sensors	Temperature, humidity, flow and pressure
Start-up time	5 minutes
Sample capture time	< 1 second
Inputs	Inbuilt tracker ball, optional connectivity to keyboard and mouse
Output	Real-time chemical spectra and stored data files for offline analysis
Characteristic (non-analysis specific)	Property
Computer	Inbuilt PC running Windows XP
Memory	4 Gb internal storage
Comms	USB × 4, RJ45 Ethernet network connection. GPIO. Bluetooth wireless (optional)
Software	Labview executable
AC Inputs	120 or 240 VAC
Dimensions	383 (w) × 262 (h) × 195 (d) mm
Weight	7.8 kg

3.3.1.1 Operation

The Lonestar system is capable of operating with just a mains electricity connection. The flow path of a Lonestar includes a heated filter from the sample inlet, pump and scrubber open to atmosphere. Figure 3.2 shows the internal flow path within the Lonestar unit, including the entry points of the carrier and sample flows. The flow within the Lonestar is maintained to a user defined level (range 0 - 2.5 l/min) via feedback between the unit's pump and proportional–integral–derivative (PID) sensor.

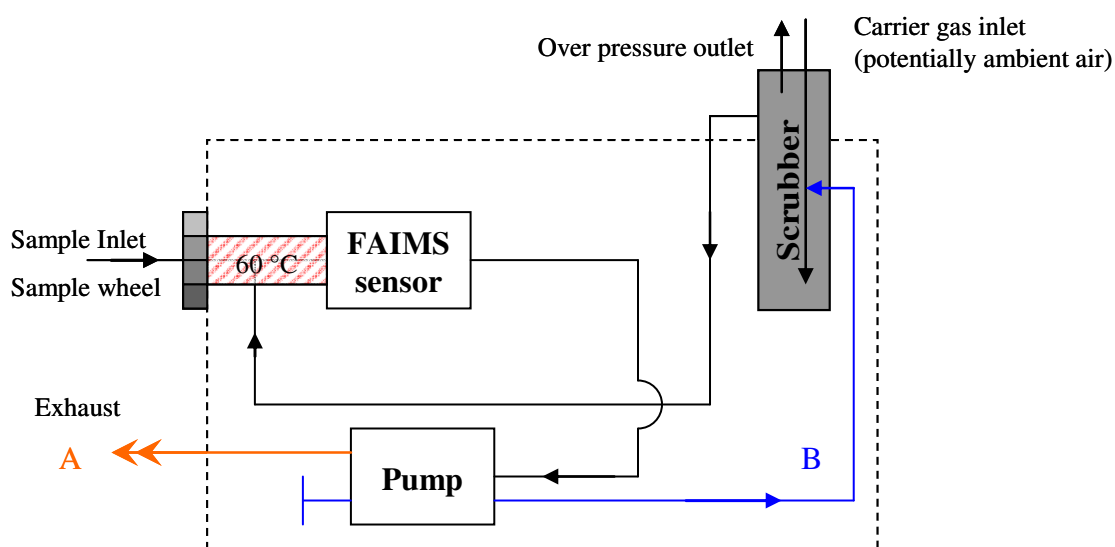


Figure 3.2 Internal flow path within a Lonestar unit. Venting mode is described by pathway A and re-circulation mode described by pathway B. The pathway in black is common to both modes.

The system is capable of operating in two modes which are suitable for different purposes.

- (1) *Venting mode*: a sample passes through the FAIMS sensor and is immediately exhausted; this is depicted in Figure 3.2 as pathway **A**. This requires a continuous volume of carrier gas to pass through the scrubber and so it is used when a clean carrier flow is connected or the likely lifetime of the scrubber is not a concern.
- (2) *Re-circulation mode*: this entails the flow being passed back to the scrubber following the pump, effectively re-circulating the carrier gas that has already passed through the FAIMS sensor, with sample being drawn in as normal. This mode does not require continuous carrier flow input and therefore extends the

lifetime of the scrubber as a smaller volume of gas is required to be cleaned; this is depicted as flow path **B** within Figure 3.2. As the pump used is not fully leak tight flow is slowly lost over the time. To ensure a constant flow is maintained the Lonestar unit will draw in additional flow through the scrubber, as in venting mode, when required. If through sampling the internal flow is too great flow will escape through the over pressure outlet on the scrubber.

Throughout the investigations within this thesis the Lonestar unit was used only in venting mode as a regulated compressed air flow was available, which was connected to the scrubber inlet. As previously described in Section 1.5 Lonestar can record data at a continuous dispersion field strength but also perform a dispersion field sweep.

Additional modifications were undertaken to Lonestar for Experiment 1 (Section 3.3.1.6).

3.3.1.2 Sample inlet

The sample inlet flow is controlled manually by setting a sample wheel; the flow through the sample inlet can be modified by choosing a larger or smaller aperture. The exact flow of the sample inlet is also dependent upon the total flow through the Lonestar unit. This is because the flow drawn through the sample inlet is a result of a pressure differential and is therefore reliant upon both quantities.

Figure 3.3 displays data from an investigation into the change in the flow of the sample inlet with each sample wheel setting across a range of total flows. The Lonestar unit flow was controlled on-board and with a PID sensor while the sample line flow was that recorded in-line using the Restek flow meter described within Section 3.2.4.

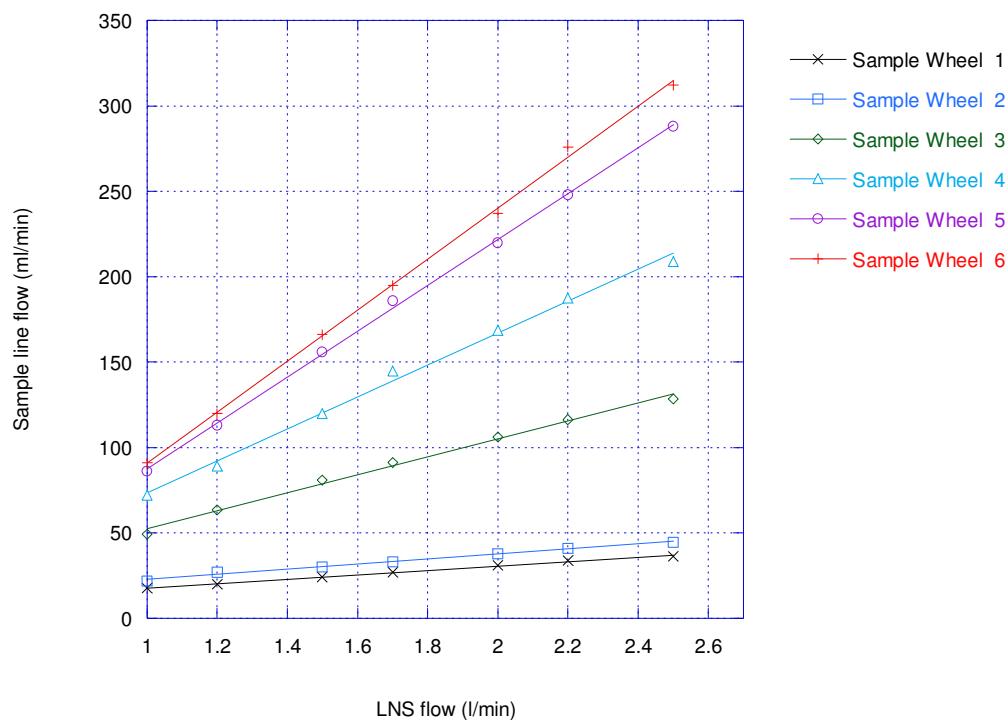


Figure 3.3 Sample line flow dependence upon sample wheel setting and total Lonestar flow

The numerical data used to construct Figure 3.3 were then used as a look-up table throughout the experiments with the Lonestar unit to allow the sample flow to be determined from the settings as opposed to disrupting flow paths to measure independently with a flow meter. Determining the sample inlet flow allowed the calculation of sample dilution within the Lonestar unit; it also verified that the flows remained within acceptable parameters. In most situations the carrier gas flow is at least an order of magnitude greater than the sample flow.

3.3.1.3 Ionisation

Ionisation within the Lonestar unit is achieved via a ^{63}Ni foil source (β radiation, activity prior to shipping 555 MBq with half-life of 100.1 years). Using a β -source means that separate gas species are not uniformly ionised; rather the process is dependent upon the proton affinity of the molecules within the reaction region. The theory behind the ionisation of air by a β source has been explored in more detail within Section 2.2.

The ^{63}Ni within the Lonestar is a closed source and so the required safety measures compared to an open source are markedly reduced. However, of concern is condensation on the source in the presence of mineral acids. This is because corrosion of the source can occur, leading to a shedding of radioactive material. In the Lonestar the radioactive source is heated to 60°C , mitigating condensation, and a filter following the ^{63}Ni foil prevents the loss of any radioactive material beyond the unit. A further safety measure is to run dry air across the source after the use of a high humidity carrier flow, as was conducted after all experimental work, to again place the system in a safe state.

3.3.1.4 Temperature control

The FAIMS sensor is maintained at $60 \pm 1^\circ\text{C}$ and also the flow path leading from the sample inlet to the FAIMS sensor is a heated filter set at $60 \pm 1^\circ\text{C}$. Apart from this there was no active control of temperature within Lonestar.

3.3.1.5 Settings

The Lonestar software allows alteration of the mode of operation (Section 3.3.1.1) and also how data was recorded. In Table 3.3, the different experimental settings and the typical setting used for each investigation is presented. Further information is given within Chapters 5 and 6, which supersedes Table 3.3 if there is disagreement.

Table 3.3 Principal relevant settings available through the Lonestar software

DF matrix setting	Possible settings	Experimental setting
Number of CV sweeps averaged	1 - 250 /off	off
Field intensity		
- linear	0 - 100%	1 - 100%
- custom	0 - 100%	-
Number of CV sweeps per full DF sweep	2 - 251	value selected so that 1 CV sweep per DF step
Process monitoring	Possible settings	Experimental setting
Number of CV sweeps averaged	1 - 250	1
Record every N th update	1 - 250	1
Instrument set-up	Possible settings	Experimental setting
Pump	on/off/auto	auto
Gas recirculation	on/off	off
Sensor heater	on/off	on
Filter heater	on/off	on
Pump PID	on/off	on
Pump voltage	0 - 10 V	- (auto pump setting controls voltage)

3.3.1.6 Owlstone FAIMS unit

In addition to the Lonestar system an Owlstone FAIMS unit was also made available for the project (Figure 3.4). The unit is simply an Owlstone FAIMS sensor (*i.e.* the same as that used in the Lonestar) with integrated ^{63}Ni ionisation source and Faraday detector. This unit does not include the additional flow paths and PC as standard within the Lonestar, there is a single inlet for both sample and carrier flow and there is no pump.

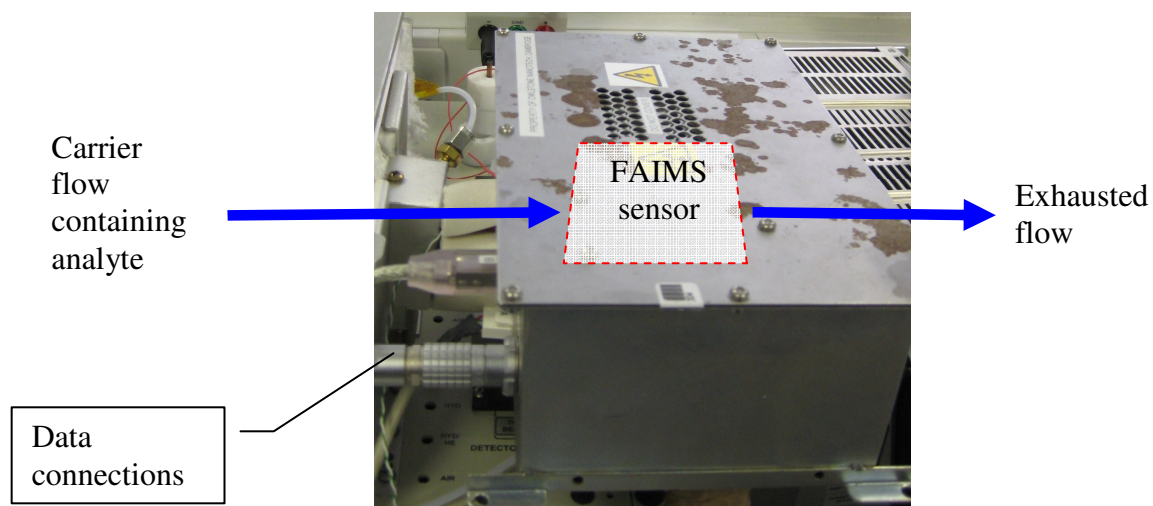


Figure 3.4 Unit housing Owlstone FAIMS sensor

This unit was used when an investigation required coupling with additional systems (*e.g.* a gas chromatograph as in Experiment 2) because its reduced size/mass meant it was more practical for the task. Furthermore, the time for data acquisition was reduced to better resolve quickly changing ion responses (*e.g.* eluting compounds from a gas chromatograph). A CV sweep (including both polarities) takes 2.8 s (2 s.f.) in a Lonestar, in the modified Owlstone FAIMS unit 1.5 s (2 s.f.) is required.

3.3.1.7 Modification for high pressure

Experiment 1 (Table 3.1) requires operation of the Lonestar at greater carrier gas pressure than it was originally designed to generate. Therefore a number of modifications had to be made. The internal flow path of the modified Lonestar is given in Figure 3.5.

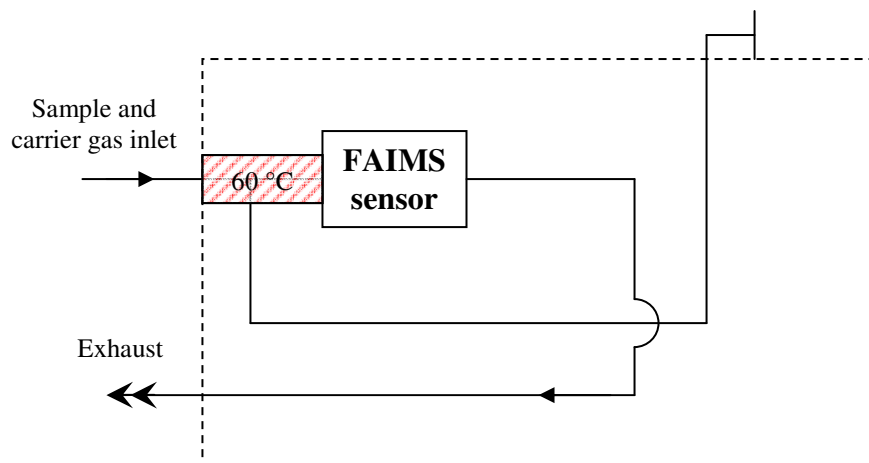


Figure 3.5 Internal flow path within a Lonestar following modification for high pressure studies.

It can be seen that the scrubber, sample wheel and pump were all removed. It should be noted that blanking off the scrubber results in a non-ideal dead volume but the stagnant flow and high flow rate through the inlets should ensure any loss of analyte (through diffusion) is minimal.

The pump was removed to ensure it would not act as any kind of restriction. The sample wheel, which under normal conditions, restricts sample flow was removed so that the full experimental flow could pass unhindered. Since all of the flow regulation previously incorporated into the Lonestar was removed, all flow control was accomplished externally.

3.3.2 Owlstone FAIMS sensor

The separation region of the Owlstone FAIMS chip is made from a serpentine shaped channel with a gap height (g) of $35\ \mu\text{m}$ and a width (w) of $115\ \mu\text{m}$ (as if the channel was not serpentine). The length (l) of the separation region is $300\ \mu\text{m}$. The dimensions are assigned in accordance with the definition from Section 2.1.

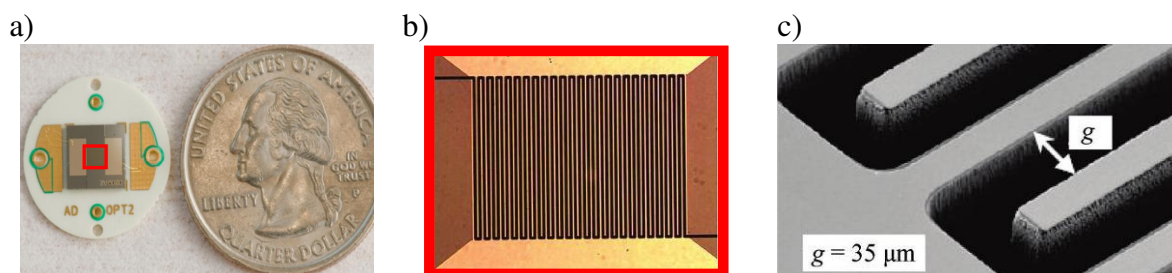


Figure 3.6 a) Owlstone FAIMS sensor chip with US quarter coin [3] b) microscope image of sensor showing serpentine channel [4] c) scanning electron microscope image of gap width [4].

The length contributed by the turns within the serpentine channel is small when compared to the straight portions of the channel (the turns contributing $< 6\%$ of total length). Thus, the sensor can be treated as a series of forty seven identical planar separation regions. The layout and characteristics of the Owlstone FAIMS sensor are included in Figure 3.7 and Table 3.4 respectively.

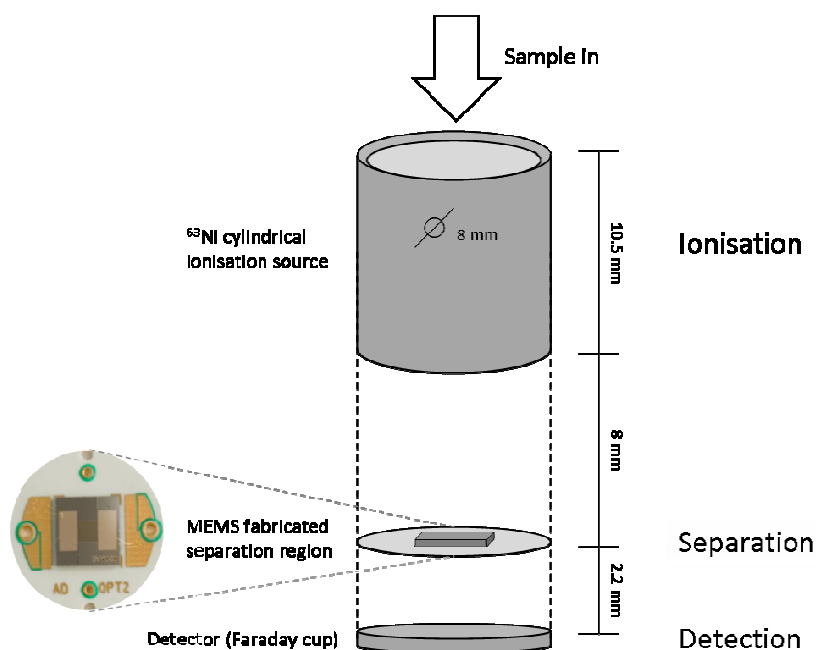


Figure 3.7 Layout of Owlstone field asymmetric ion mobility spectrometer in relation to ionisation and detection regions.

Table 3.4 Summary of the characteristics of the Lonestar FAIMS sensor

Characteristic	Quantity
Max voltage _{p-p}	360 V
Frequency	28 MHz
Duty cycle	25%
Sensor temperature	60 °C
Dimensions of separation region	
- gap height	35 μm
- width	115 mm
- length	300 μm
- N ^o of channels	47

3.3.3 Gas chromatography (GC)

Gas chromatography is an analytical separation technique used primarily to resolve mixtures of volatile chemicals; these are injected into the apparatus, vapourised and then separated as they migrate over an adsorbent (stationary phase) whilst carried by an inert gas (mobile phase) [5]. Individual species are retarded due to their unique interaction with

the stationary phase along the pathway and are carried along with the mobile phase. The individual species therefore elute at different times from the end of the flow path.

3.3.3.1 SRI gas chromatograph

The GC used within Experiment 2 (Table 3.1) was the 8610C gas chromatograph available through SRI Instruments (California, USA) shown within Figure 3.8.

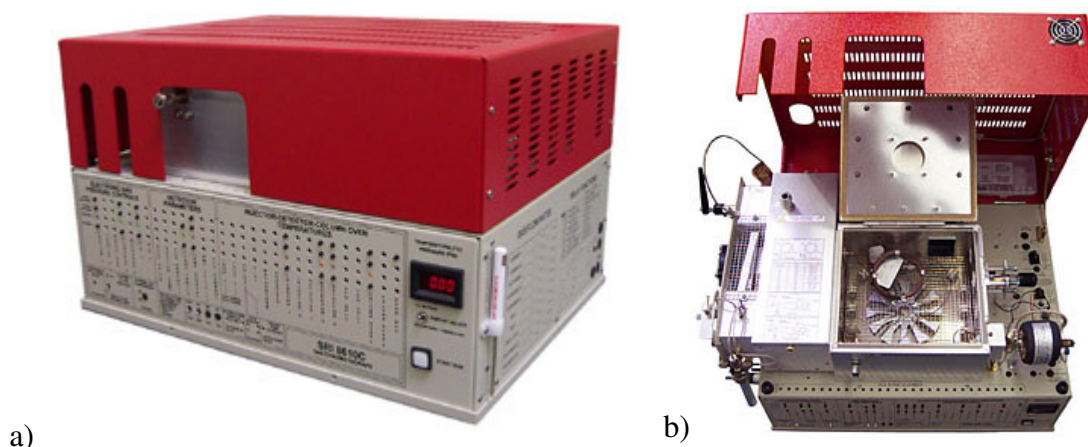


Figure 3.8 The SRI-GC electronics and pneumatic controls are housed within the lower half of the instrument while the GC oven, injectors and detectors are housed under the red hood.

The system is capable of multiple configurations but for the work undertaken here the sample introduction was through splitless injection (SureFit split/splitless, Restek). Two columns were used for the experimentation: MXT-5 (15 m × 0.25 mm × 1 μm, Restek) and BP-624 (30 m × 0.25 mm × 25 μm, SGE). The former being a low polarity metal column principally designed for separating different explosives and has a low column bleed [6]. This phenomenon, where the stationary phase being shed from the column due to the continuous elevated temperatures and flow, is always desired to be as small as possible; otherwise it provides an increase in the baseline signal obtainable from any attached detecting system. The other column was chosen for its polar stationary phase, which promotes increased separation of polar compounds.

For Experiment 2, in place of a standard GC detector (*e.g.* flame ionisation device, electron capture device) an Owlstone FAIMS unit (Section Figure 3.4) was used. The relevant configuration can be seen in Figure 3.9. A Swagelok 1/8" stainless steel Tee (SS-200-3) was positioned between the GC outlet and FAIMS inlet to allow the column from the GC oven to be fed into the ionisation region of the FAIMS unit. The Tee-piece allowed the carrier gas (supplied through an Owlstone mass flow controller) to enter the FAIMS unit along with the eluting compounds from the GC.

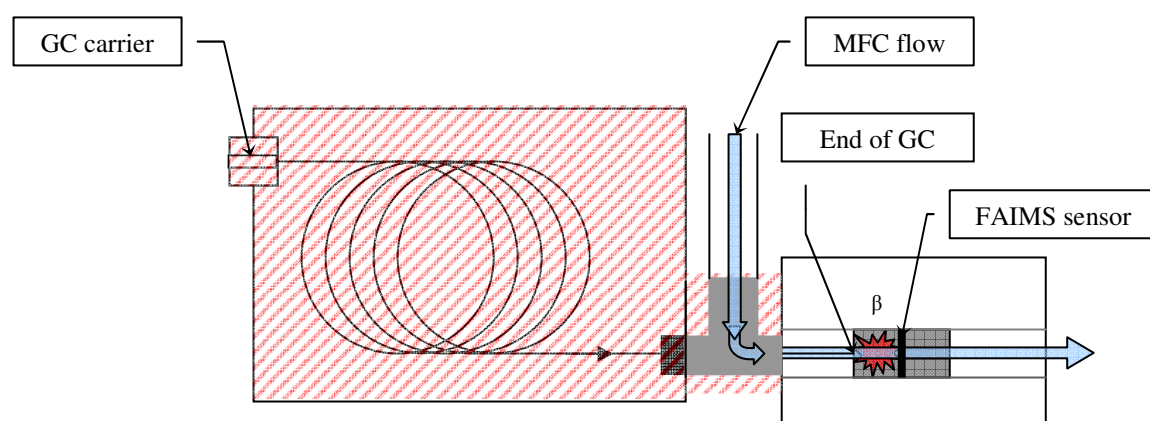


Figure 3.9 Schematic illustrating the union between the SRI-GC and the flow path of the FAIMS PAD unit. Red stripes denote where active heating was applied.

The end of the gas chromatograph column was placed in close proximity (~ 0.5 cm) to the ionisation region of the FAIMS unit. Neutral carrier gas entered the flow path upstream of the end of the chromatography column which aided transportation of the eluting compounds into the FAIMS sensor. External heating, by heated wire, was controlled by an independent power supply. A full summary of the experimental parameters is provided in Section 3.6.

3.4 Techniques for sample introduction

Through the work detailed in this thesis a sample introduction method other than gas chromatography was used; namely permeation sources. Permeation sources have their own benefits and drawbacks and these will be discussed in the following section.

3.4.1 Permeation sources

The operation of a permeation source (PS) is shown in Figure 3.10; typically it is used to produce a constant, low concentration of analyte (ppm - ppb) within a gaseous flow. This is achieved by housing a sample of liquid analyte within a gas permeable chamber, which is basically a tube with a headspace. The permeation source is then kept within a heated chamber, through which passes a flow of clean and dry gas.

PSs used in this thesis were constructed in-house from, 1/4" outer diameter and 1/5" inner diameter, PTFE and plugs made from PTFE rod (outer diameter 1/4"). Magnetic stainless steel crimps were used to secure the plugs, which also allowed easy retrieval of a permeation source from an oven by the use of a magnetic rod. Figure 3.10 is a labelled schematic of the permeation tubes constructed. Due to limitations of the oven dimensions the maximum length of the permeation sources used was 18 cm.

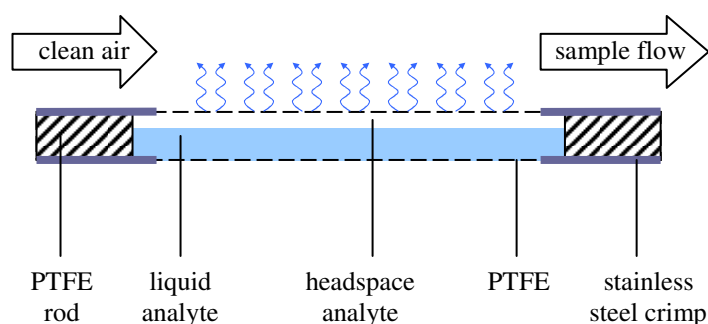


Figure 3.10 A permeation source with components listed

Within the PS, liquid and gas phases reach a dynamic equilibrium which is dependent upon the vapour pressure of the analyte; gases from the headspace are then able to diffuse through the walls of the permeation source and into the flow passing over the source within the heated chamber. As long as the temperature of the chamber does not change, the permeation rate of analyte from the PS remains constant. The flow of carrier gas along with trace concentrations of analyte is then directed for study.

Gravimetric measurements of a permeation source at a given temperature are used to determine the permeation rate. The permeation rate is dependent upon the surface area of the PS holding the analyte, vapour pressure of analyte and the temperature at which the permeation source is held at. The flow over the permeation source must be constant and high enough to adequately remove any permeated analyte so that a constant concentration gradient across the permeation source wall is maintained. The rate of the flow over the permeation source also determines the analyte concentration within the sample flow.

The change in mass (Δm), of a permeation source is discovered gravimetrically by:

$$\Delta m = m_i - m_f . \quad 3.1$$

Where m_i is the initial mass and m_f is the final mass.

The permeation rate (PR) is found from the change in mass divided by the time taken for the mass change recorded to occur:

$$\text{PR} = \frac{dm}{dt} = \frac{\Delta m}{t_{ml}} . \quad 3.2$$

Where t_{ml} is the time taken for the recorded mass loss to occur.

The concentration of analyte within the sample flow ($[c]$ by mass/volume) is obtained by dividing the permeation rate by the flow rate of the clean air passing over the permeation source:

$$[c] = \frac{PR}{F_{PS}} \quad 3.3$$

Where F_{PS} is the flow rate of the clean air that passed over the permeation source.

To maintain the temperature and flow rate of the PS an electronic controller was used (Owlstone vapour generator (OVG), Figure 3.11). Regular gravimetric readings were taken of the permeation sources (± 0.2 mg, BEL Engineering) and the sources were not used until they were shown to generate a constant permeation rate. It was empirically determined that sources take approximately a day to stabilise following a temperature change. The OVGs also incorporated a split flow capability allowing for a larger range of analyte concentrations to be created. Technical specifications of the OVGs used are given in Table 3.5.



Figure 3.11 Owlstone vapour generator (OVG) 4.

Table 3.5 Technical specifications of Owlstone vapour generator [7].

Characteristic	Property
Technology	Permeation tube
Inlet	1/4" Swagelok quick connector
Outlet	1/8" Swagelok compression fittings
Output concentrations	ppb - ppm
Instrument air	Regulated air / nitrogen at 40 psi free from impurities, - 35°C dew point
Sample flow	50 - 500 ml/min
Split flow	1000 ml/min
Oven warm-up	15 min to 100°C (stable ± 0.1 °C)
Permeation oven temperature	35 - 100 °C
Permeation oven diameter	10 mm
Permeation oven length	180 mm
Power supply	24 VDC
Current	6 A
Dimensions	h 262 mm, w 142 mm, d 260 mm
Weight	4.55 kg

Figure 3.12 provides the mass loss over time of different compounds from permeation sources of the same size. The data was collected gravimetrically and demonstrates that the permeation sources created and deployed in OVGs displayed consistent mass losses over prolonged periods; error bars are a single standard deviation of triplicate readings.

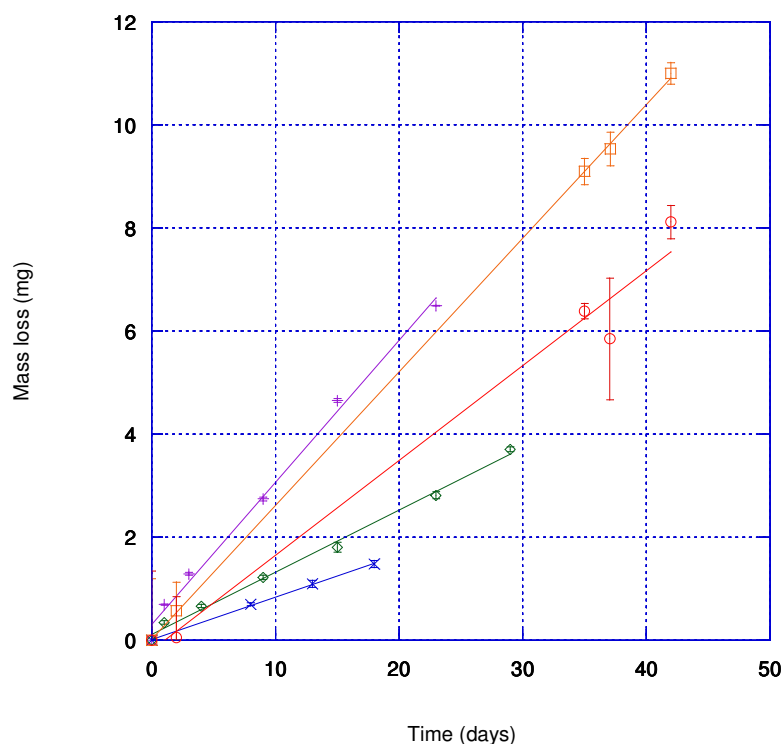


Figure 3.12 Mass loss of several permeation sources as used within an Owlstone vapour generator, OVG (chloroform at 50°C - Purple, ethyl benzene at 60°C - Blue, bromoform at 60°C - Green, DMMP at 80°C - Orange and DEEP at 80°C - Red).

Appendix G gives details of a study that was undertaken to develop a theoretical model that could provide an estimate of the rate of permeation for an individual PS. The aim was for this estimation to be created from easily obtainable quantities such as molecular mass and vapour pressure of the analyte. The eventual result of the work was the appreciation that to obtain a rigorous estimation, a number of difficult to attain parameters had to be discovered first. Such parameters were often easiest to acquire experimentally. The experimental time could alternatively be used to directly measure the permeation rate of a constructed PS, undermining the justification for a predictive model and making any estimated result obsolete as the true value could be acquired.

3.5 CASE STUDY 1: Detection of dimethylmethylphosphonate

(Experiment 1)

Experiment 1 was designed to investigate the influences of varying the properties of pressure, humidity and magnitude of flow upon the detection of dimethylmethylphosphonate (DMMP) by the Owlstone FAIMS sensor. The concentration of analyte delivered to the sensor was required to be constant; therefore a permeation source was employed. Also, because the pressure of the flow was required to reach values greater than ambient a Lonestar unit modified for such work (Section 3.3.1.7) was employed.

3.5.1 Experimental set-up and parameters

Figure 3.13 a) describes the flow path constructed to undertake Experiment 1 and Figure 3.13 b) is a picture of the equipment as it was set up in the laboratory.

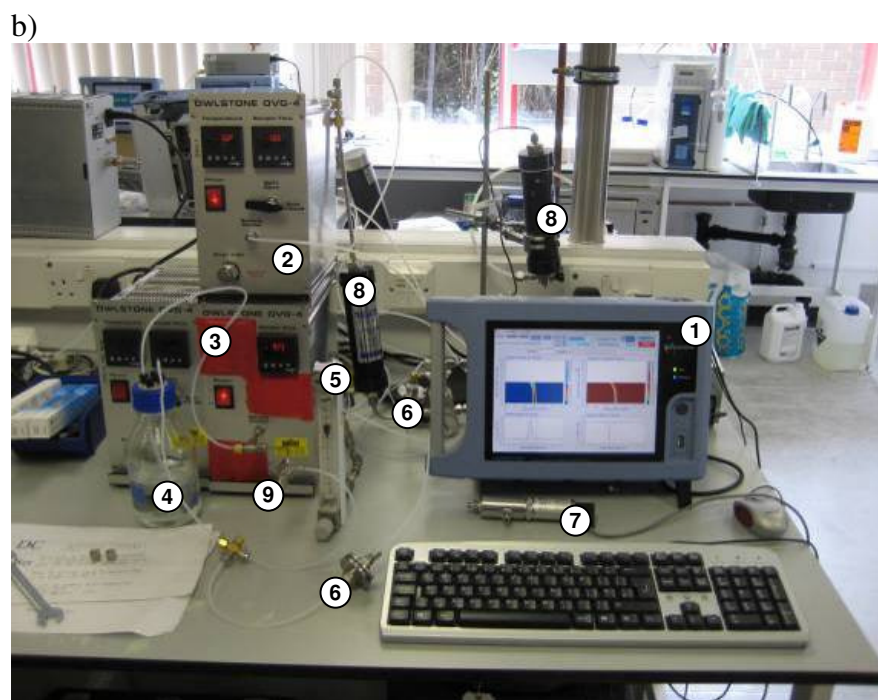
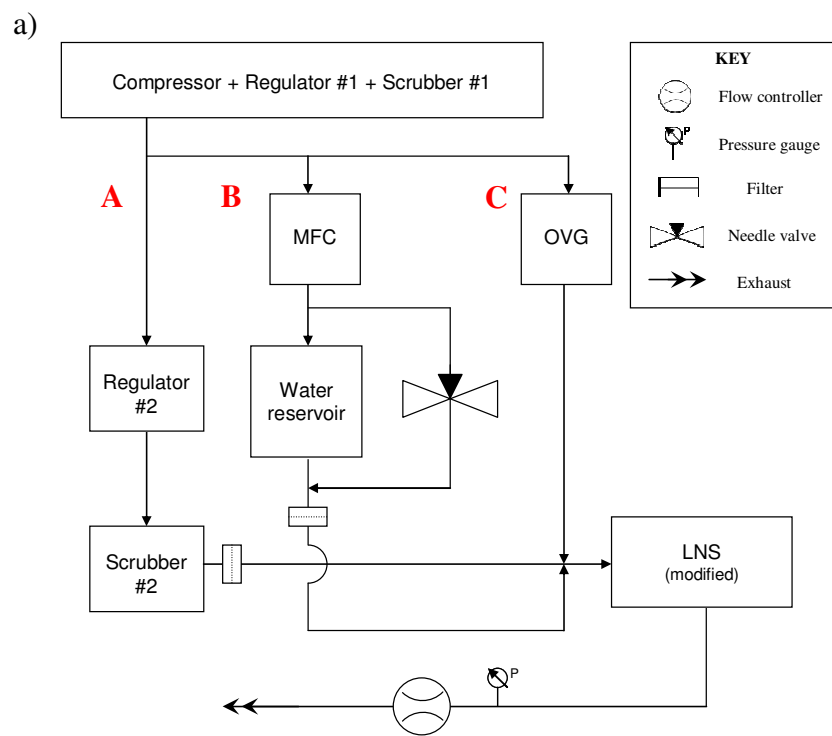


Figure 3.13 a) Flow path of Experiment 1, flow paths **A**, **B** and **C** eventually combine prior to the Lonestar unit, b) photograph of apparatus used for Experiment 1. (1) Lonestar, (2) OVG, (3) MFC, (4) water reservoir, (5) flow controller, (6) filters, (7) humidity sensor, (8) scrubbers and (9) needle valve. Remaining components not pictured.

Table 3.6 contains the experimental parameters as set through Experiment 1.

Table 3.6 Experimental parameters of Experiment 1

Experimental parameter	Value
Flow A : carrier	1500 - 2500 ml/min air
Flow B : humidity	250 ml/min air
Flow C : analyte	100 ml/min air
Filter: pore size	1 μm
Humidity	Variable, 10 to 5500 ppm
Pressure: carrier	120 - 200 kPa

The inlet into the modified Lonestar unit comprised of a carrier gas flow (**A**), humidifying flow (**B**) and analyte flow (**C**) (Figure 3.13 a)). All three flows originated from the laboratory's compressed air source (regulated and cleaned of volatiles and humidity) which was then split. The carrier flow was then further regulated and passed through a second scrubber for volatiles. This additional regulator was required to ensure that any modification of the carrier flow would not affect the other flows during testing.

The humidifying flow was managed by a mass flow controller. Independent pathways allowed the humidifying flow to (1) bubble through and (2) flow through a dry line, further controlled via a needle valve. The total humidifying flow was constant, but the fraction of the flow passing through the water reservoir could be varied, which allowed the level of humidity to be adjusted without affecting the total flow entering the Lonestar.

The sample flow passed through an OVG containing a DMMP permeation source maintained at 50°C, resulting in a permeation rate of 14.4 ng/min (3 s.f.), and flow of 100 ml/min.

The total flow through the Lonestar was controlled by a flow controller on the exhaust of the unit while the pressure was controlled by the regulator on the carrier gas flow (A). The pressure directly downstream of the Lonestar was monitored via the pressure gauge prior to the flow meter on the Lonestar exhaust. Filters were also installed following the water reservoir and scrubber of the humidifying and carrier gas flows to prevent entry of water droplets and dust into the Lonestar.

3.5.2 Blank response

Between investigations the humidity and analyte flows were disconnected from the Lonestar inlet to allow clean and dry air to continuously purge the system. Prior to measurement, several full DF sweeps were completed to assess whether there was any contamination within the spectra. One such blank response obtained from Experiment 1 is given in Figure 3.14.

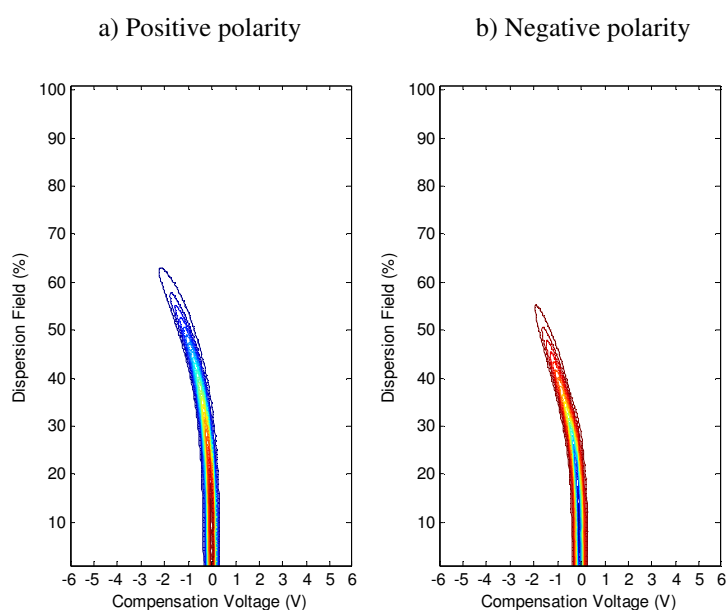


Figure 3.14 Blank DF sweeps from Experiment 1, (a) positive and (b) negative mode are both displayed.

Data in Figure 3.14 shows the typical response of a clean system; the observed ion responses are a result of H_3O^+ (hydronium ions) and hydrated O_2^- ions and together are referred to as the reactant ions (as a result of the presence of N_2 and O_2 molecules within the carrier flow respectively). The eventual data from Experiment 1 was taken at specific field strengths (Chapter 4) therefore it was useful to confirm that there was no indication of contamination within the CV sweeps at representative field strengths. Figure 3.15 shows the CV sweeps of the blank response, *i.e.* reactive ion peak (RIP), in the positive mode at dispersion field strengths of 10, 30 and 50%.

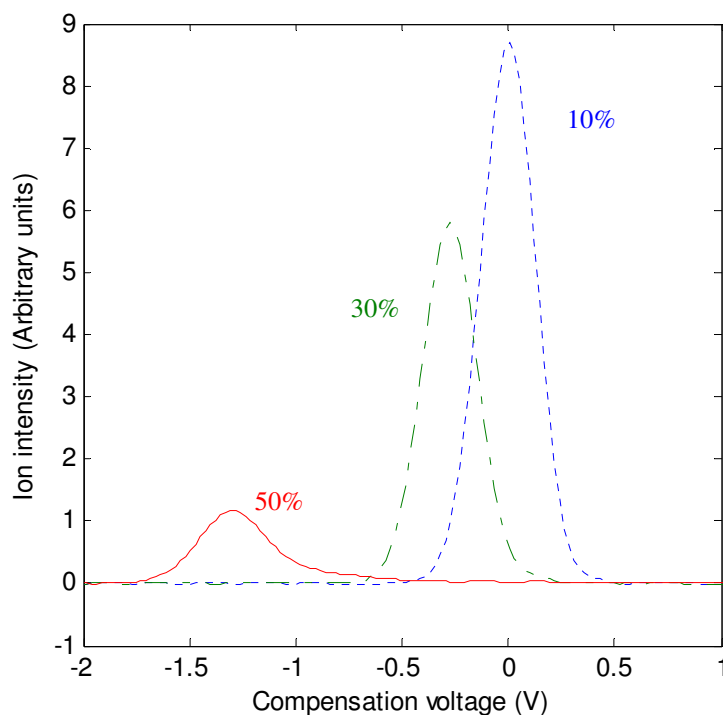


Figure 3.15 The RIP from the positive mode at DF strengths of 10, 30 and 50%.

Any asymmetry within a FAIMS response would suggest the presence of ion species other than the hydronium ions. In order to assess this for the data in Figure 3.15 Gaussian peaks were fitted. In order to assess how well the fitted curve describes the data coefficients of determination were obtained:

$$R^2 = \frac{\sum (y_i - f_i)^2}{\sum (y_i - \bar{y})^2} \quad 3.4$$

Where y_i are the data points, \bar{y} is the mean of the data points and f_i are the points of the fitted curve. An R^2 value of one (*i.e.* $R = 1$) indicates that the fitted Gaussian peak perfectly describes the curve.

R^2 values of 0.99966, 0.99984 and 0.98125 were obtained for DF strengths of 10, 30 and 50% respectively. This indicated that there was very little variation of the ion responses from perfect Gaussian peaks and further supports that the blank response was a clean one.

3.5.3 Stability

There is also the possibility that with ions continuously entering and impacting upon the FAIMS sensor that charging can occur, resulting in a drift in observed spectra. Any charge on the sensor is lost when the software is stopped (since the sensor is not provided with an electric field) and this was scheduled following every third DF sweep at any given condition during Experiment 1.

Figure 3.16 shows two CV spectra, in the presence of analyte, at the same dispersion field taken five DF sweeps apart.

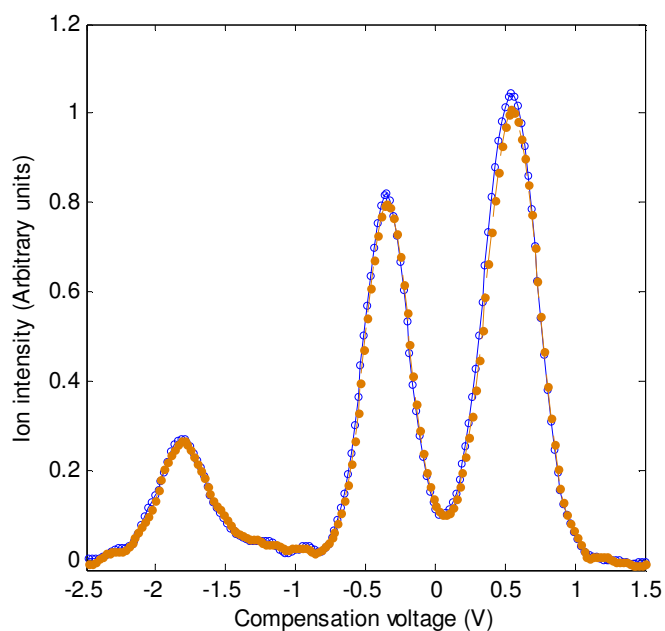


Figure 3.16 Two CV sweeps from Experiment 1 in the presence of analyte. CV sweeps were obtained five full DF sweeps apart.

There is variation between the two data sets and in terms of compensation voltage displacement it appears to be small, displacement is by a single CV increment. The CV position and peak intensity of the three major peaks during the five successive DF sweeps at identical field settings are provided within Figure 3.17; error bars are a single standard deviation of triplicate readings.

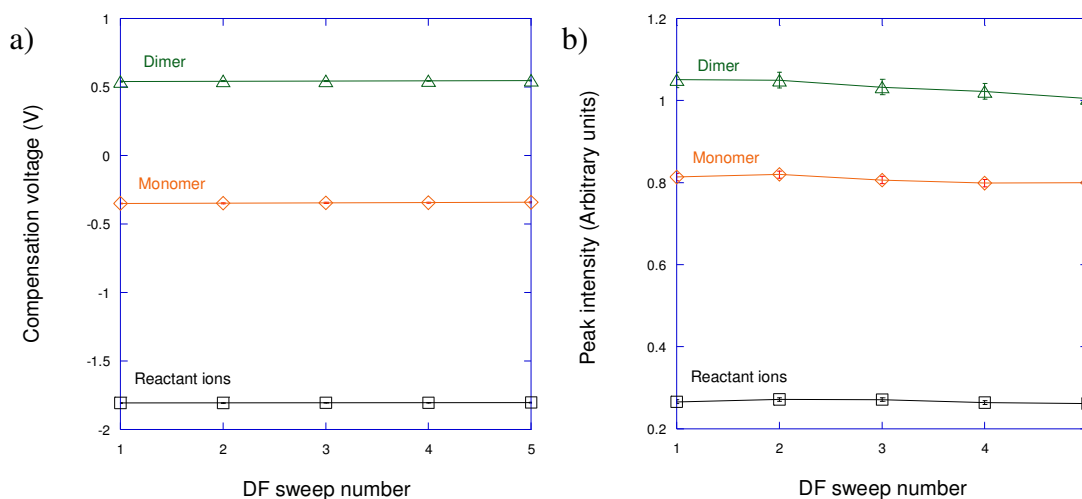


Figure 3.17 a) Compensation voltages of five DF sweeps carried out under identical conditions (lines by least square fit) b) peak intensity of five DF sweeps carried out under identical conditions. Errors are single standard deviation, otherwise smaller than data icon.

The CV drift across all five DF sweeps is of the order of ± 1 increment and suggests that through the period of operation there is no large scale variation during data acquisition within Experiment 1. The peak intensity of the three main ion responses displays greater variation and appears dependent upon the species identity. The deviation is, however, not dramatic and it is proposed that the system is stable. To quantify the variation with this apparatus, during the full investigation, triplicates with standard deviations were taken.

3.6 CASE STUDY 2: Detection of ethyl acetate within wine (Experiment 2)

Experiment 2 was designed to investigate the potential of a FAIMS sensor as a detector for gas chromatography. The system was configured to provide both ambient and elevated pressures of carrier flow to the FAIMS unit.

3.6.1 Experimental set-up and parameters

Figure 3.18 a) shows the flow paths used in the undertaking of Experiment 2 and Figure 3.18 b) is a picture of the equipment as it was set up in the laboratory during an experimental run.

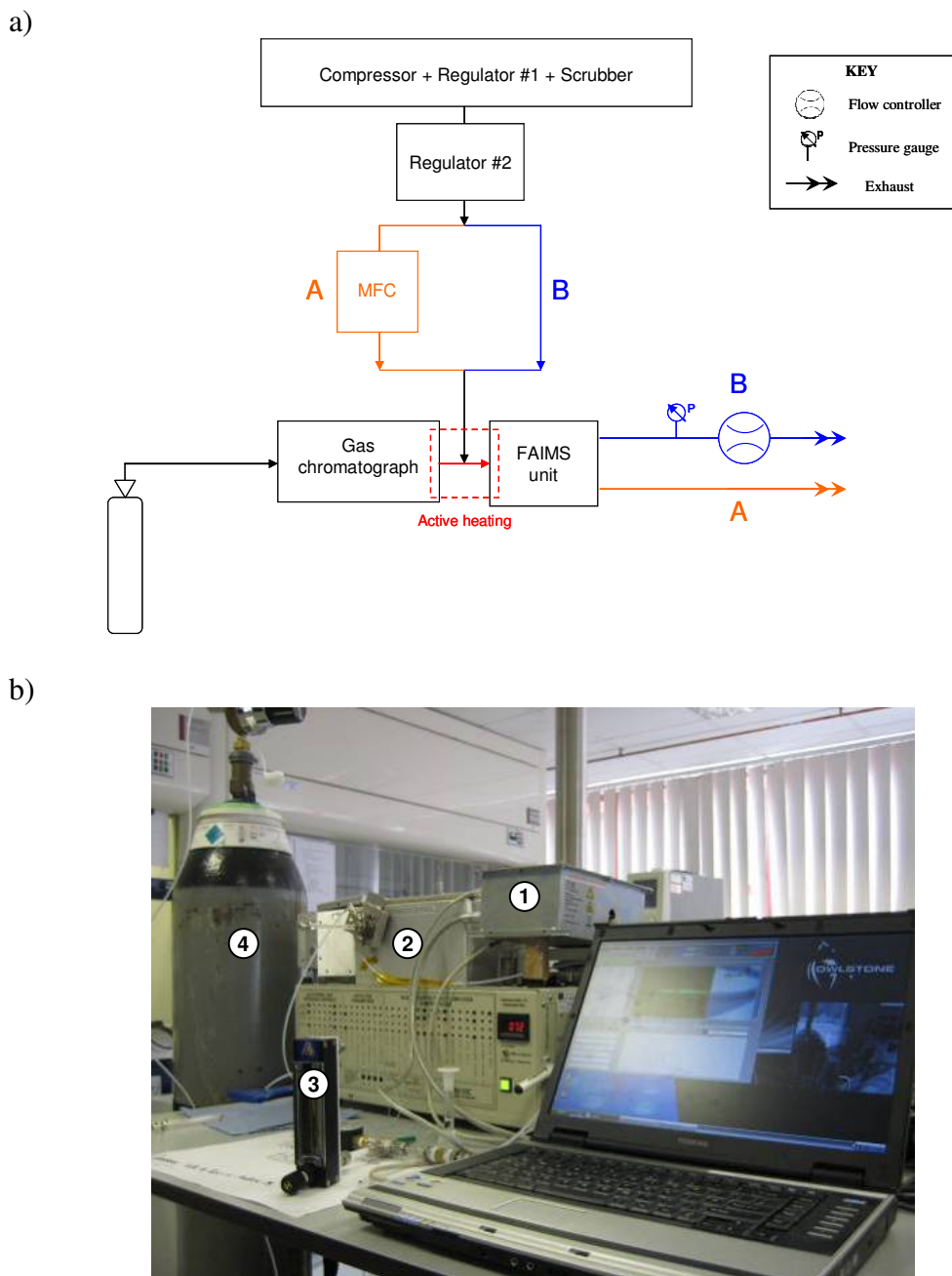


Figure 3.18 a) Flow path of Experiment 2. There are two configurations denoted by **A** and **B**. The A configuration is used for experiments where the pressure through the FAIMS unit is ambient. The B configuration is used for investigations where the pressure above ambient is required in the FAIMS unit. Red pathway is heated. b) Photograph of apparatus used in Experiment 2. (1) FAIMS unit, (2) GC, (3) flow controller and (4) N₂ cylinder. Remaining components not pictured.

Table 3.7 contains the experimental parameters as set through Experiment 2.

Table 3.7 Experimental parameters of Experiment 2

Experimental parameter	Value
Flow: carrier	2.75 l/min air
Flow: GC	1.5 ml/min N ₂
Pressure: carrier	Atmospheric + variable
Pressure: GC	14 psi across column
Temperature: GC	70°C isothermal
Temperature: union	120 °C
GC injection	Splitless
GC column	MXT-5 (15 m × 0.25 mm × 1 μm) or BP-624 (30 m × 0.25 mm × 1.4 μm)

The flow through the GC (1.5 ml/min) was provided by a N₂ cylinder while the carrier gas to the FAIMS unit (2.75 l/min) was provided by the laboratory compressed air supply. The union between the GC and FAIMS unit has been described previously within Section 3.3.3.1 and was maintained at a temperature of 120°C. The FAIMS unit simply included the Lonestar sensor with a ⁶³Ni ionisation source and Faraday detector (Section 3.3.1.6). It did not incorporate a pump, heated filter or additional sensors (*e.g.* humidity, temperature).

When elevated pressures were required the flow was controlled by a flow controller (used as a restriction) on the exhaust of the FAIMS unit. The pressure of the carrier gas within the FAIMS unit was controlled by manipulation of Regulator #2 and monitored by the pressure gauge on the exhaust of the FAIMS unit.

3.6.2 Blank response

Figure 3.19 shows a contour fill plot for an example blank response from Experiment 2, taken at ambient pressure and a constant DF strength of 38% of the maximum electric field strength. As the product ions of interest in the study were exclusively in the positive polarity only the positive mode is considered here. The most obvious feature in the plot is that there are two prominent responses. The largest and most negative in CV position is suggested as a result of reactive ions while the second response (nearer zero CV) is attributed to the column bleed from the gas chromatograph.

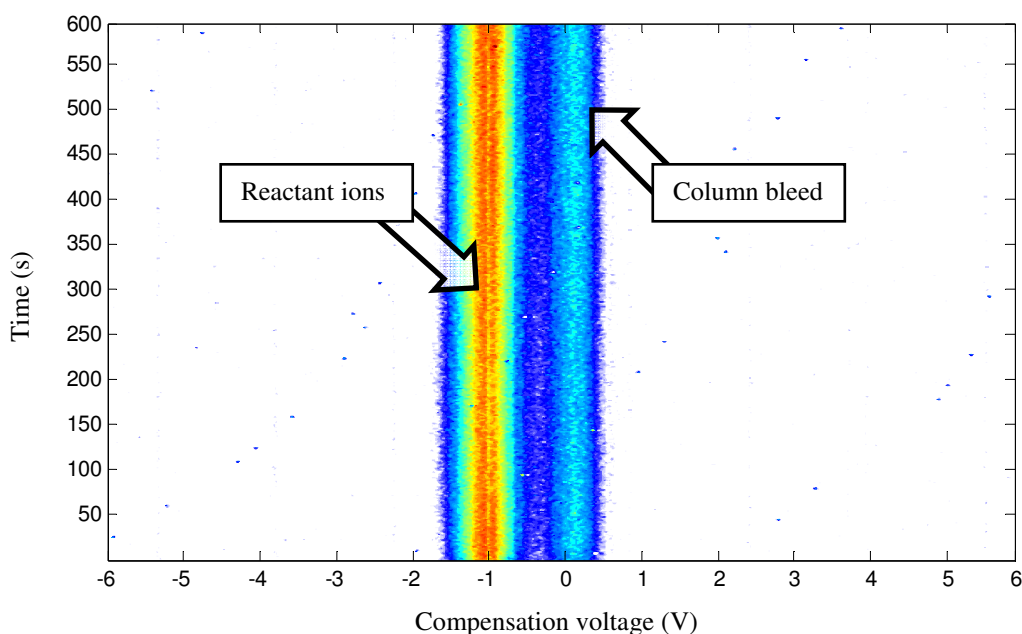


Figure 3.19 Contour fill plot of the blank response from the GC-FAIMS unit operated at ambient pressure.

Figure 3.20 displays two baseline-corrected (later described in Chapter 4) CV sweeps at the start and end of the blank response. There is little difference between the two CV sweeps indicating that the spectra are stable and no large variation results through continuous operation. There is a decreased signal-to-noise ratio, compared to previous experiments, and this is suggested to be a consequence of the column bleed entering the FAIMS unit and shorter time for data acquisition for each CV sweep (Section 3.3.1.6). The R^2 of the responses (Section 3.5.2) from the reactant ions and column bleed was found to

be 0.95326 and 0.84206, respectively. This suggests that there is some asymmetry within the ion responses. This may be an effect of the low signal-to-noise ratio, meaning random fluctuations are having an effect upon the peak shapes. It is also likely that the presence of the column bleed means that there are a number of additional ion species from the shedding of the GC column. However, the asymmetry is still quite low indicating that the ion responses are the result of dominant ion species for both the reactant ions and column bleed.

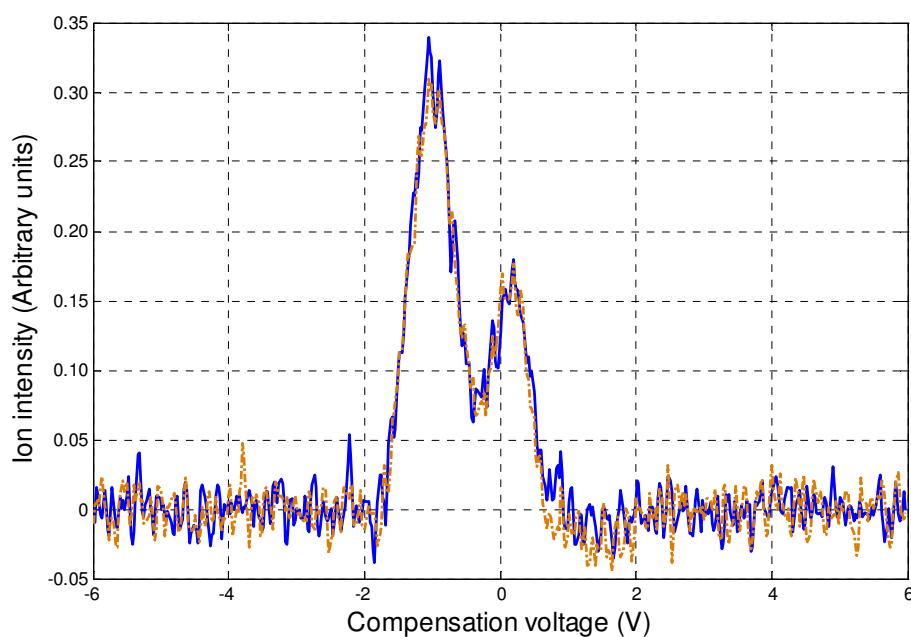


Figure 3.20 CV sweeps taken at the beginning of the blank run (blue solid) and near the end (orange dot-dash).

The CV position and peak intensity of the peak ion response within a CV sweep (nominally the peak of reactant ion response) across a blank run are shown in Figure 3.21. The blank run was greater in length than used in the full investigation.

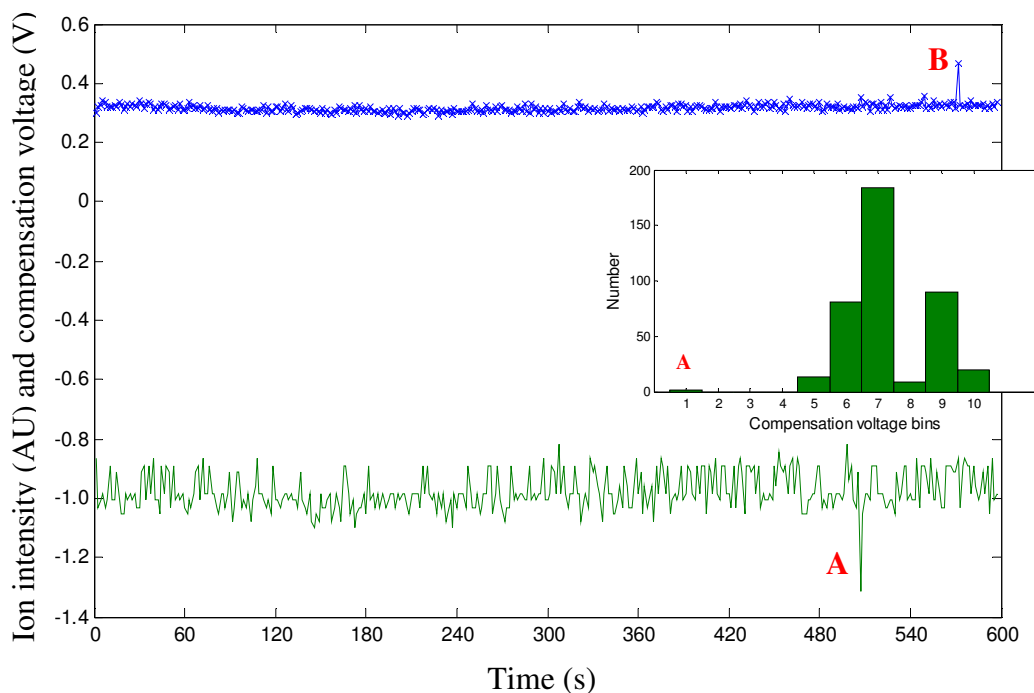


Figure 3.21 CV positions (solid green) and peak intensity (blue crosses, solid line) of the peak ion response within CV sweep during a blank run of Experiment 2. **A** and **B** have been highlighted for discussion. Inset is a histogram of the CV positions.

There appears to be no consistent drift over time in either the CV position or peak intensity. Compounds of interest within the full investigation are also expected to elute from the GC column in a time much shorter than the 600 s shown above. The standard deviation of the CV position and peak intensities recorded were 0.0622 V and 0.0134 respectively. These values will help inform the later interpretation of errors in the full investigation. A histogram of the CV positions obtained has also been included as it more clearly demonstrates that there is a binomial distribution within the series. This was attributed to the presence of more than a single population of ions within what is typically described as the RIP.

Of note are two features highlighted as **A** and **B** within Figure 3.21. Typically the CV position and peak intensity was consistent but these two features appear to be events that

have randomly occurred. Further investigation was possible by studying the two CV sweeps where **A** and **B** occur, as presented in Figure 3.22.

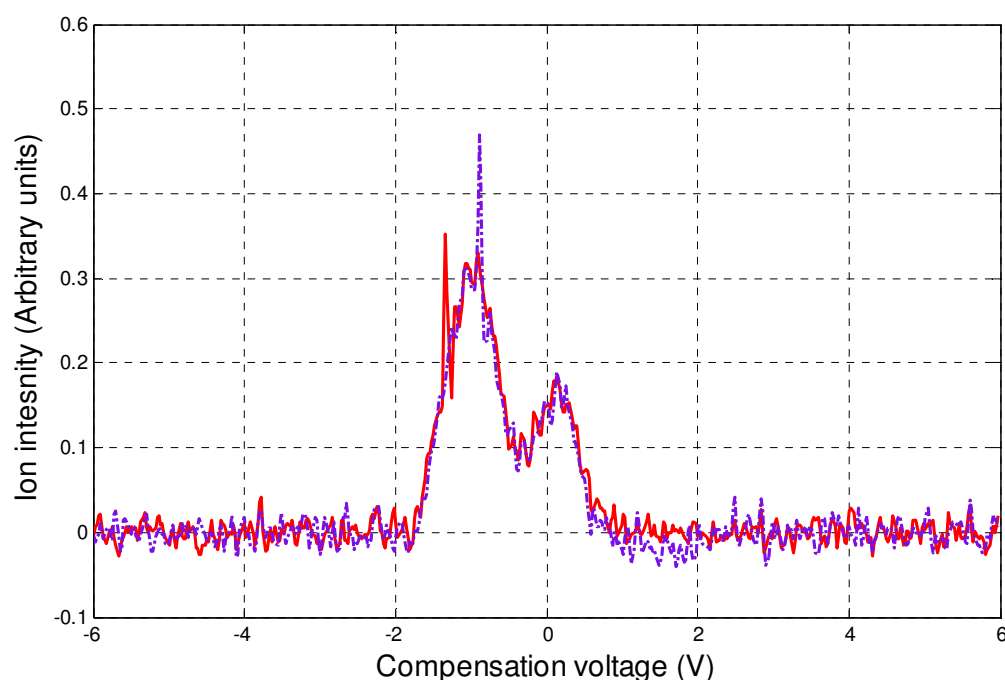


Figure 3.22 CV sweeps corresponding to features highlighted in Figure 3.21. Red solid from feature **A** and purple dot-dash from feature **B**.

Events **A** and **B** appear to be independent of one another and are the result of a sudden and localised incident. Given the large FWHM associated with ion responses from FAIMS this issue appears to be related to software where a single data entry has been augmented for some reason. Both events occur over half way through the extended run which suggests that their occurrence is more likely the longer the system is in operation. There is clearly some (but not major) instability within the system that cannot be predicted and is a possible consequence of running the CV sweeps at a faster rate (Section 3.3.1.6). To counter this, in the full investigation (Chapter 6), an average of repeated runs will be taken to mitigate against the effects of these events. Following this it was deemed that the blank responses from Experiment 2 were stable and well understood.

3.7 References

1. Golay, M.J.E. *Gas Chromatography*. in *Gas Chromatography*. 1958. Amsterdam, Netherlands: Butterworths, London.
2. Owlstone_Ltd. *Lonestar, Field Asymmetric Ion Mobility Spectrometer*. 2010 [cited Aug 2010]; Available from: http://www.owlstonenanotech.com/PDF/Lonestar_2Pager.pdf.
3. Owlstone_Ltd. *Owlstone Nanotech website*. 2009 [cited; Available from: <http://www.owlstonenanotech.com/>].
4. Shvartsburg, A.A., Smith, R.D., Wilks, A., Koehl, A., Ruiz-Alonso, D., and Boyle, B., *Ultrafast Differential Ion Mobility Spectrometry at Extreme Electric Fields in Multichannel Microchips*. *Analytical Chemistry*, 2009. **81**(15): p. 6489–6495.
5. Hinshaw, J.V. and Ettre, L.S., *Introduction to Open-Tubular Column Gas Chromatography*. 1994 Edition ed. 1994, Cleveland, Ohio: Advanstar Communications. 161.
6. Rush, M. and Parris, R., *MXT-5 gas chromatography column bleed*, A. Morris, Editor. 2010: Cambridge, UK.
7. Owlstone_Ltd. *OVG-4 Technical Specifications*. 2010 [cited 2010 Aug 2010]; Available from: <http://www.owlstonenanotech.com/site.php?ovg>.